

See discussions, stats, and author profiles for this publication at: <https://www.researchgate.net/publication/50319134>

# Onsager Revisited: Magnetic Field Induced Nematic–Nematic Phase Separation in Dispersions of Goethite Nanorods

ARTICLE *in* JOURNAL OF PHYSICAL CHEMISTRY LETTERS · JULY 2010

Impact Factor: 7.46 · DOI: 10.1021/jz100707f · Source: OAI

CITATIONS

14

READS

53

6 AUTHORS, INCLUDING:



**Esther Van den pol**

Shell Global

23 PUBLICATIONS 225 CITATIONS

SEE PROFILE



**Andrei V Petukhov**

Utrecht University

175 PUBLICATIONS 2,519 CITATIONS

SEE PROFILE



**Dmytro Byelov**

Utrecht University

43 PUBLICATIONS 651 CITATIONS

SEE PROFILE



**Gert Jan Vroege**

Utrecht University

66 PUBLICATIONS 2,181 CITATIONS

SEE PROFILE

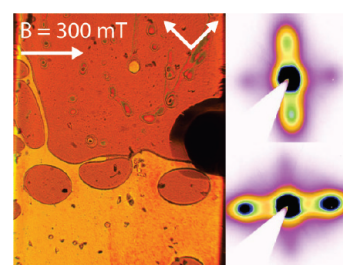
# Onsager Revisited: Magnetic Field Induced Nematic–Nematic Phase Separation in Dispersions of Goethite Nanorods

E. van den Pol,<sup>†</sup> A. Lupascu,<sup>‡,¶</sup> M. A. Diaconeasa,<sup>‡</sup> A. V. Petukhov,<sup>†</sup> D. V. Byelov,<sup>†</sup> and G. J. Vroege<sup>\*,†,‡</sup>

<sup>†</sup>Van 't Hoff Laboratory for Physical and Colloid Chemistry, Debye Institute for Nanomaterials Science, Utrecht University, Padualaan 8, 3584 CH Utrecht, The Netherlands, and <sup>‡</sup>University College Utrecht, Utrecht University, Campusplein 1, 3584 ED Utrecht, The Netherlands

**ABSTRACT** We found, using polarization microscopy and small-angle X-ray scattering, that for goethite, a low polydispersity suffices to form two separate nematic phases, while previous theory showed that this is only possible for mixtures of particles with extremely different lengths or diameters. Applying a critical magnetic field, which induces some of the goethite nanorods to rotate, leads to sufficient excluded volume between the particles to cause macroscopic phase separation between two orthogonal nematic phases. The larger the polydispersity of the system, the broader the range of field strengths where nematic–nematic phase separation occurs. This is a new phase separation mechanism which is expected to lead to interesting interfacial phenomena.

**SECTION** Macromolecules, Soft Matter



Sixty years ago, Onsager published his seminal paper on the first purely entropy-driven phase transition.<sup>1</sup> He described the transition from the disordered isotropic (I) phase to the orientationally ordered nematic (N) phase in terms of the excluded volumes between anisometric particles. Another, much more rare, effect is N–N phase separation in systems with extremely different lengths or diameters, where, to leading order, the excluded volume does not play a role.<sup>2–11</sup>

Onsager formulated a simple virial expansion of the free energy for dispersions of both rodlike and platelike particles. The expansion can be truncated after the second virial term for infinitely thin, hard rods. The free energy  $F$  per particle, in units of the thermal energy  $kT$ , is then given by<sup>1,12</sup>

$$\frac{\Delta F}{NkT} \approx \text{constant} + \langle \ln(\rho f) \rangle + \frac{1}{2} \rho \langle \langle v_{\text{excl}} \rangle \rangle \quad (1)$$

where  $\rho \equiv N/V$  is the number density of rods and  $\langle \ln(\rho f) \rangle$  is a combination of the ideal translational and orientational entropy. Each pair of triangular brackets denotes an average in terms of the relevant particle angles described by orientational distribution function  $f$ . The packing entropy is proportional to the excluded volume ( $v_{\text{excl}}$ ), asymptotically given by

$$v_{\text{excl}} \approx 2DL^2 |\sin \gamma| \quad (2)$$

with  $\gamma$  as the angle between two thin rods of diameter  $D$  and length  $L$ . The I–N phase transition is explained as a shifting balance between the orientational and packing entropy (Figure 1). At a certain concentration, the gain in packing entropy will exceed the loss in orientational entropy, and the system will undergo an I–N phase transition. Remarkably,

within the nematic phase, the average excluded volume between particles is found to be

$$\langle \langle v_{\text{excl}} \rangle \rangle \approx 4/\rho \quad (3)$$

At higher concentrations, the particles spontaneously align more strongly, thus reducing the excluded volume so that the last term in eq 1 remains constant.

Comparing these theoretical results with experiments, polydispersity is an important factor. Interestingly, eqs 1 and 3 remain valid if the triangular brackets now also include (number) averaging over the different particle dimensions and the excluded volume is generalized to include different lengths and diameters.<sup>13</sup> The first numerical results on bidisperse systems were presented by Lekkerkerker et al., showing strong fractionation effects and widening of the biphasic I–N gap.<sup>14</sup>

Another remarkable effect found in bidisperse systems is the occurrence of N–N phase separation.<sup>2–11</sup> To better understand this phenomenon, an analytical theory was used.<sup>4–6</sup> Surprisingly, the excluded volume does not play a role here since the last term of eq 1 remains constant within the nematic phase; instead, the phenomenon involves the balance between the orientational entropy and the entropy of mixing. The long particles induce a too strong alignment of the short particles, whose orientational entropy favors demixing. Typically, a large length ratio of at least 3.2 or a diameter

Received Date: May 26, 2010

Accepted Date: June 29, 2010

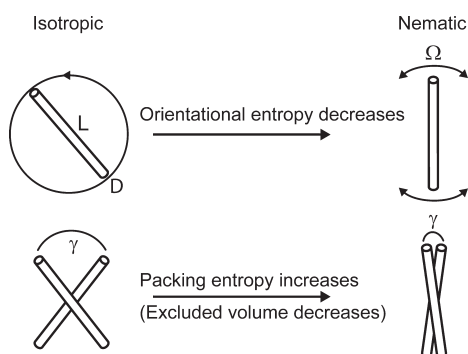


**Figure 1.** Isotropic to nematic phase transition.

**Table 1.** Critical Field Measurements

system	$\langle L \rangle$	$\sigma_L$ (%)	$\langle W \rangle$	$\sigma_W$ (%)	$\langle T \rangle$	$(B_c - B_{\text{limit}})/B_c$ (%)
g55	216	55	35	48	$\sim 16$	51
g29	242	29	49	30	$\sim 17$	35
g14	189	14	57	25	$\sim 17$	22

ratio of 4.3 is needed to get N–N phase separation.<sup>8</sup> Later, it was shown that N–N phase separation can also be obtained in a polydisperse system<sup>15–17</sup> and for more realistic  $L/D$  ratios.<sup>9–11</sup> Experimentally, this effect has been observed in bidisperse,<sup>18</sup> bimodal,<sup>19</sup> and polydisperse systems.<sup>20</sup>

The I–N phase transition in a magnetic field has been studied before.<sup>21–23</sup> In this work, the nematic phase itself is studied in a magnetic field. We use repulsive goethite particles, which are boardlike (in between rod- and platelike). When dispersed in water, their surface charge leads to somewhat larger effective particle dimensions. More concentrated goethite dispersions readily show nematic, smectic, and columnar phases.<sup>24–26</sup> The magnetic properties of these particles are very intriguing.<sup>24</sup> They have a permanent magnetic moment  $\vec{\mu}$  along their longest axis  $L$ , presumably because of uncompensated surface spins within their antiferromagnetic crystal structure. In contrast, the magnetic easy axis of magnetic susceptibility tensor  $\vec{\chi}$  lies along the shortest particle dimension  $T$ . Therefore, the particles align parallel to a weak and perpendicular to a stronger magnetic field.

The magnetic energy ( $E_m$ ) per particle in a magnetic field  $\vec{B}$  is given by<sup>27</sup>

$$E_m = -\vec{\mu} \cdot \vec{B} - \frac{V}{2\mu_0} \vec{B} \cdot \vec{\chi} \cdot \vec{B} \quad (4)$$

with  $V$  as the particle volume. In dilute systems, this gives a Boltzmann distribution with  $E_m$  in the exponent,<sup>27</sup> so that an orientational distribution function can be externally imposed. Near the I–N phase boundary, the magnetic energy (eq 4) should be added (in units of  $kT$ ) to the free energy (eq 1).<sup>28</sup>

We prepared vertical samples of the g29 system (Table 1) showing I–N phase separation (Figure 2a; for details see Supporting Information), focusing our studies on the nematic phase. Polarization microscopy was used to study its behavior in a magnetic field. Without the magnetic field, the nematic phase showed domains with different orientations (Figure 2a). When a small magnetic field (a few mT up to 180 mT) was

applied, the particles aligned parallel to the field, and a homogeneous nematic phase was observed (Figure 2b). Increasing to the critical field strength (300 mT), where particles change their orientation from parallel to perpendicular to the field, a fine texture was formed immediately (Figure 2c). The fine texture consisted of small droplets of apparently different phases. The droplets readily coalesced and grew over time (Figure 2d). Two types of droplets formed; one kind moved upward and the other downward (Figure 2e). After about a day, macroscopic phase separation was reached, and an interface was formed between the two nematic phases (Figure 2f). Besides that, a rise of the level of the I–N interface was observed. Interestingly, previous measurements seem to indicate an alternative escape mechanism where a striped pattern of different domains of a single phase at oblique angles to the magnetic field is being formed.<sup>29</sup>

To determine the nature of the different nematic phases, small-angle X-ray scattering (SAXS) was performed at the DUBBLE beamline<sup>30</sup> of the ESRF using the microradian setup (see Supporting Information).<sup>31</sup> Before applying a magnetic field, nematic domains with different orientations were observed. Immediately after applying a field of 270 mT, perpendicular to the X-ray beam, two orthogonal orientations were recognized everywhere in the nematic phase (Figure 3a). The sample was kept in this field for about a day and was studied with polarized light microscopy. During this day, phase separation within the nematic phase was again observed (Figure 3b). SAXS patterns at different heights within the nematic phase are shown in Figure 3c–g. It can be seen that above the interface (c,d), the particles were oriented parallel to the field; the broad peaks originated from the correlations between the smaller particle dimensions. Below the interface (f,g), the particles were aligned perpendicular to the field. At the interface (e), both particle orientations were observed since the beam hit both nematic phases.

Subsequently, a 270 mT field was applied along the X-ray beam (Figure 4), thereby realigning the particles. In the upper nematic phase, the particles immediately aligned along the new direction of the field; therefore, one looks on top of the particles with the X-ray beam. A uniform scattering ring was obtained (Figure 4a), implying that this nematic phase was uniaxial. In the lower nematic phase, the long axis of the particles aligned perpendicular to the field. The observed scattering peaks are due to the correlations between the two smallest particle dimensions. The scattering patterns with the field perpendicular to the beam (Figure 3f,g) have their peaks at a larger angle or smaller correlation distance than the pattern with the field parallel to the X-ray beam (Figure 4b). This implies that the smallest correlation distance is along the field direction, in accordance with an easy axis of magnetization along  $T$  (for a schematic picture, see Figure 4c). The lower phase is therefore a biaxial nematic phase.

It can be concluded that the phase separation within the initially uniform nematic phase is based on perpendicular particle orientations which are imposed by an external field. Within the critical magnetic field range, some particles already start to orient perpendicular to the field, while other particles are still aligned parallel to the field. In this way, these two extreme types of particles experience a maximum

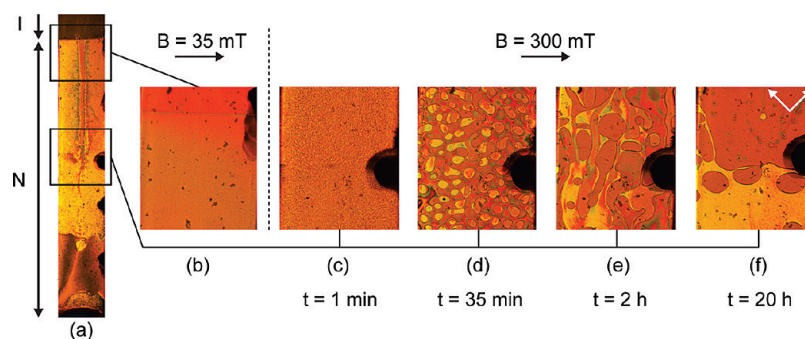


**Figure 2.** Polarized light microscopy pictures of (a) an I–N phase-separated sample ( $g29$ ,  $\phi = 9\%$ ) without a magnetic field, (b) alignment in a field of 35 mT, (c) the nematic phase with a fine texture in a magnetic field of 300 mT at  $t = 1$  min, (d) growing droplets at  $t = 35$  min, (e) droplets moving at  $t = 2$  h, and (f) phase separation at  $t = 20$  h. The black areas are marks to recognize the position in the sample. The width of the images is 1 mm (= width of the capillary).

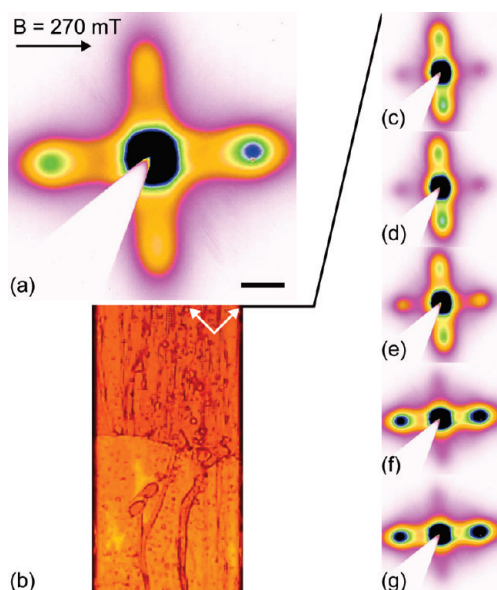


**Figure 3.** SAXS patterns of the nematic phase in a magnetic field of 270 mT, perpendicular to the X-ray beam, (a) just after applying the field and (c,d) after 1 day above the formed interface (e) at the interface and (f,g) below the interface. The scale bar is  $0.05 \text{ nm}^{-1}$ . (b) The (low-resolution) polarized light microscopy picture corresponding to (c–g). The width of the capillary is 2 mm ( $g29$ ,  $\phi = 11.5\%$ ).

excluded volume ( $\gamma = 90^\circ$ ; see Figure 1 and eq 2) and will therefore gain a lot of packing entropy by phase separating into two nematic phases with different orientations. Particles with an intermediate orientation seem to end up in either one of the two orthogonal phases. A different mechanism is causing this N–N phase separation than what was found before;<sup>18–20</sup> in those examples, the excluded volume did not play a large role.

In calculations for monodisperse particles, field-induced N–N phase separation could not be identified (private communication, H.H. Wensink);<sup>28</sup> therefore, polydispersity might play an important role in the process. First of all, larger particles tend to align perpendicular at a lower field strength compared to that for smaller particles since the permanent and induced moments depend on the particle size in a different manner. Furthermore, a polydispersity in the permanent magnetic

moment is even expected for monodisperse particles because the number of uncompensated surface spins within the anti-ferromagnetic structure is not necessarily the same for every particle.

To determine the effect of polydispersity on N–N phase separation, systems with different size polydispersities have been studied. The particle dimensions of the systems studied can be found in Table 1. The behavior of the nematic phase of these systems was studied within a range of field strengths using polarized light microscopy.

For the  $g29$  system, the first signs of phase separation were observed at a field strength of 185 mT, as can be seen from the small areas of a different phase at the bottom of the capillary in Figure 5a. In the first stage of the phase separation process, droplets started to form at the bottom of the capillary. This is already an indication that the larger particles rotate at this small field because larger particles will be mainly present at the bottom of the capillary due to sedimentation.

The larger the field, the larger the lower phase with the orientation of the particles perpendicular to the field, as can be observed in Figure 5b and c. At 300 mT (b), almost half of the nematic phase has the perpendicular orientation, and at 500 mT (c), there are only some droplets with the parallel orientation left which are slowly moving upward within the nematic phase. This is expected because by increasing the field, more particles will start to orient perpendicular to the field.

To make a comparison between the systems with different polydispersities, first the critical field ( $B_c$ ) of the isotropic phase (fresh samples with a volume fraction of 5%) was determined. This was done by finding the field where the isotropic phase became dark again (between crossed polarizers) after first becoming bright at lower fields. This is the field where the order parameter is zero. At lower fields, it is positive because of the parallel alignment of the particles, and at higher fields, it is negative due to the perpendicular alignment. Then, for I–N phase separated samples, the field was established where the first signs of N–N phase separation were observed ( $B_{\text{limit}}$ ). The difference between the two values ( $B_c - B_{\text{limit}}$ ) is a measure of the range of field strengths where N–N phase separation takes place. Measuring this directly was not possible because smectic and/or columnar phases formed before a full nematic phase was reached, which changed the composition of the nematic phase.<sup>32</sup> The ratio  $(B_c - B_{\text{limit}})/B_c$  is compared with the



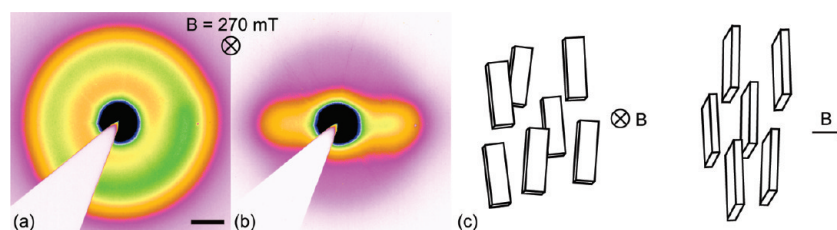


**Figure 4.** SAXS patterns of the nematic phase in a magnetic field of 270 mT, parallel to the X-ray beam, (a) after 1 day above the formed interface and (b) below the formed interface. The scale bar is  $0.05 \text{ nm}^{-1}$ . (c) Schematic picture of the lower nematic phase with two directions of the magnetic field.

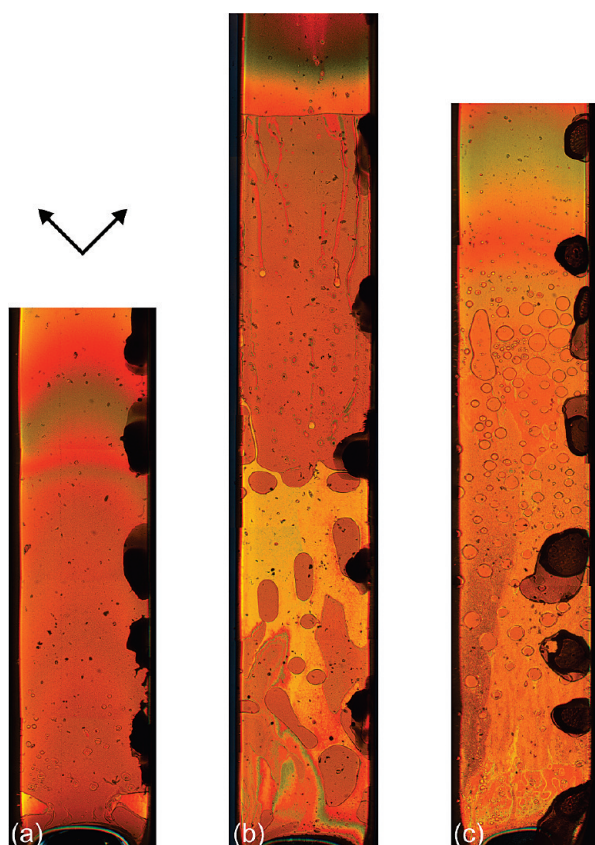


**Figure 5.** Polarization microscopy pictures of N–N phase-separated samples of the g29 system at (a) 185, (b) 300, and (c) 500 mT ( $\phi = 9.5$ , 9, and 10%, respectively). The width of the capillaries is 1 mm.

polydispersity in Table 1. There is a clear relation between this ratio and the polydispersity of the systems; the values are even comparable. This indicates that the polydispersity of the particles has a large influence on the N–N phase separation process.

In summary, we showed that phase separation takes place inside of the nematic phase of colloidal goethite dispersions within the critical field range where individual particles change orientation. SAXS measurements proved that the two resulting nematic phases have orthogonal orientations, a uniaxial nematic with particles parallel to the field and a biaxial nematic with particles perpendicular to the field. The occurrence of N–N phase separation in this system is remarkable because it was previously found that a large length ratio between particles is needed to get N–N phase separation.<sup>8</sup> In our case, a different

mechanism is causing the phase separation because an external magnetic field causes the orientational distribution function to broaden and even leads to orthogonal orientations. The phase separation is then rationalized by the large excluded volume between these perpendicularly oriented particles. Polydispersity is an important factor for N–N phase separation since the magnetic properties of the particles depend on their size. It was found that the larger the polydispersity of the system, the broader the range of field strengths where N–N phase separation occurs. The interface formed between these phases is extremely interesting since the two orthogonal orientations have to join there. As can be observed from Figure 2, the interfacial tension between the phases seems to be remarkably low (cf. ref 33), and droplets are not spindle-shaped as often observed with I–N interfaces. Different kinds of coalescence events are observed during phase separation, which is the subject of further studies.

**SUPPORTING INFORMATION AVAILABLE** Experimental details are included. This material is available free of charge via the Internet at <http://pubs.acs.org>.

## AUTHOR INFORMATION

### Corresponding Author:

\*To whom correspondence should be addressed. E-mail: [g.j.vroege@uu.nl](mailto:g.j.vroege@uu.nl)

### Present Addresses:

<sup>†</sup> Condensed Matter Physics, University of Toronto, 60 St. George St., Toronto, Ontario, Canada M5S 1A7.

**ACKNOWLEDGMENT** This work is part of the research program SFB TR6 of the Stichting voor Fundamenteel Onderzoek der Materie (FOM), which is financially supported by the Nederlandse Organisatie voor Wetenschappelijk Onderzoek (NWO) and Deutsche Forschungsgemeinschaft (DFG). The work of A.L. was supported by a Schlumberger grant. We thank P. Davidson for enlightening discussions. We also thank the staff of the BM26 DUBBLE beamline at ESRF for their excellent support and Th. Narayanan for sharing the magnet.

## REFERENCES

- (1) Onsager, L. The Effects of Shape on the Interaction of Colloidal Particles. *Ann. N.Y. Acad. Sci.* **1949**, *51*, 627–659.
- (2) Abe, A.; Flory, P. J. Statistical Thermodynamics of Mixtures of Rodlike Particles. 2. Ternary Systems. *Macromolecules* **1978**, *11*, 1122–1126.

- (3) Birshtein, T. M.; Kolegov, B. I.; Pryamitsyn, V. A. Theory of Athermal Lyotropic Liquid Crystal Systems. *Polym. Sci. U.S.S.R.* **1988**, *30*, 316–324.
- (4) Vroege, G. J.; Lekkerkerker, H. N. W. Theory of the Isotropic–Nematic–Nematic Phase Separation for a Solution of Bidisperse Rodlike Particles. *J. Phys. Chem.* **1993**, *97*, 3601–3605.
- (5) van Roij, R.; Mulder, B. Demixing Versus Ordering in Hard-Rod Mixtures. *Phys. Rev. E* **1996**, *54*, 6430.
- (6) van Roij, R.; Mulder, B. Absence of High-Density Consolute Point in Nematic Hard Rod Mixtures. *J. Chem. Phys.* **1996**, *105*, 11237–11245.
- (7) van Roij, R.; Mulder, B.; Dijkstra, M. Phase Behavior of Binary Mixtures of Thick and Thin Hard Rods. *Physica A* **1998**, *261*, 374–390.
- (8) Hemmer, P. C. Phase Transitions in a Solution of Rodlike Macromolecules of Two Different Sizes. *Mol. Phys.* **1999**, *96*, 1153–1157.
- (9) Varga, S.; Galindo, A.; Jackson, G. New Types of Phase Behaviour in Binary Mixtures of Hard Rod-like Particles. *Mol. Phys.* **2003**, *101*, 817–825.
- (10) Wensink, H. H.; Vroege, G. J. Demixing in Binary Mixtures of Anisometric Colloids. *J. Phys.: Condens. Matter* **2004**, *16*, S2015.
- (11) Varga, S.; Purdy, K.; Galindo, A.; Fraden, S.; Jackson, G. Nematic–Nematic Phase Separation in Binary Mixtures of Thick and Thin Hard Rods: Results from Onsager-like Theories. *Phys. Rev. E* **2005**, *72*, 51704.
- (12) Vroege, G. J.; Lekkerkerker, H. N. W. Phase Transitions in Lyotropic Colloidal and Polymer Liquid Crystals. *Rep. Prog. Phys.* **1992**, *55*, 1241–1309.
- (13) Odijk, T. Osmotic Pressure of a Nematic Solution of Polydisperse Rod-like Macromolecules. *Liq. Cryst.* **1986**, *1*, 97–100.
- (14) Lekkerkerker, H. N. W.; Coulon, P.; Van Der Haegen, R.; Deblieck, R. On the Isotropic–Liquid Crystal Phase Separation in a Solution of Rodlike Particles of Different Lengths. *J. Chem. Phys.* **1984**, *80*, 3427–3433.
- (15) Speranza, A.; Sollich, P. Isotropic–Nematic Phase Equilibria of Polydisperse Hard Rods: The Effect of Fat Tails in the Length Distribution. *J. Chem. Phys.* **2003**, *118*, 5213–5223.
- (16) Speranza, A.; Sollich, P. Isotropic–Nematic Phase Equilibria in the Onsager Theory of Hard Rods with Length Polydispersity. *Phys. Rev. E* **2003**, *67*, 61702.
- (17) Wensink, H. H.; Vroege, G. J. Isotropic–Nematic Phase Behavior of Length-Polydisperse Hard Rods. *J. Chem. Phys.* **2003**, *119*, 6868–6882.
- (18) Purdy, K. R.; Varga, S.; Galindo, A.; Jackson, G.; Fraden, S. Nematic Phase Transitions in Mixtures of Thin and Thick Colloidal Rods. *Phys. Rev. Lett.* **2005**, *94*, 57801.
- (19) Itou, T.; Teramoto, A. Triphase Equilibrium in Aqueous Solutions of the Rodlike Polysaccharide Schizophyllan. *Macromolecules* **1984**, *17*, 1419–1420.
- (20) Buining, P. A.; Lekkerkerker, H. N. W. Isotropic–Nematic Phase Separation of a Dispersion of Organophilic Boehmite Rods. *J. Phys. Chem.* **1993**, *97*, 11510–11516.
- (21) Tang, J.; Fraden, S. Magnetic-Field-Induced Isotropic–Nematic Phase Transition in a Colloidal Suspension. *Phys. Rev. Lett.* **1993**, *71*, 3509.
- (22) van der Beek, D.; Davidson, P.; Wensink, H. H.; Vroege, G. J.; Lekkerkerker, H. N. W. Influence of a Magnetic Field on the Nematic Phase of Hard Colloidal Platelets. *Phys. Rev. E* **2008**, *77*, 031708.
- (23) Lemaire, B. J.; Davidson, P.; Ferré, J.; Jamet, J. P.; Petermann, D.; Panine, P.; Dozov, I.; Stoenescu, D.; Jolivet, J. P. The Complex Phase Behavior of Suspensions of Goethite ( $\alpha$ -FeOOH) Nanorods in a Magnetic Field. *Faraday Discuss.* **2005**, *128*, 271–283.
- (24) Lemaire, B. J.; Davidson, P.; Ferré, J.; Jamet, J. P.; Panine, P.; Dozov, I.; Jolivet, J. P. Outstanding Magnetic Properties of Nematic Suspensions of Goethite ( $\alpha$ -FeOOH) Nanorods. *Phys. Rev. Lett.* **2002**, *88*, 125507.
- (25) Vroege, G. J.; Thies-Weesie, D. M. E.; Petukhov, A. V.; Lemaire, B. J.; Davidson, P. Smectic Liquid-Crystalline Order in Suspensions of Highly Polydisperse Goethite Nanorods. *Adv. Mater.* **2006**, *18*, 2565–2568.
- (26) Lemaire, B. J.; Davidson, P.; Panine, P.; Jolivet, J. P. Magnetic-Field-Induced Nematic–Columnar Phase Transition in Aqueous Suspensions of Goethite ( $\alpha$ -FeOOH) Nanorods. *Phys. Rev. Lett.* **2004**, *93*, 267801.
- (27) Lemaire, B. J.; Davidson, P.; Ferré, J.; Jamet, J. P.; Petermann, D.; Panine, P.; Dozov, I.; Jolivet, J. P. Physical Properties of Aqueous Suspensions of Goethite ( $\alpha$ -FeOOH) Nanorods: Part I: In the Isotropic Phase. *Eur. Phys. J. E* **2004**, *13*, 291–308.
- (28) Wensink, H. H.; Vroege, G. J. Nematic Order of Model Goethite Nanorods in a Magnetic Field. *Phys. Rev. E* **2005**, *72*, 31708.
- (29) Lemaire, B. J.; Davidson, P.; Petermann, D.; Panine, P.; Dozov, I.; Stoenescu, D.; Jolivet, J. P. Physical Properties of Aqueous Suspensions of Goethite ( $\alpha$ -FeOOH) Nanorods: Part II: In the Nematic Phase. *Eur. Phys. J. E* **2004**, *13*, 309–319.
- (30) Bras, W.; Dolbnya, I. P.; Detollenaere, D.; van Tol, R.; Malfois, M.; Greaves, G. N.; Ryan, A. J.; Heeley, E. Recent Experiments on a Combined Small-Angle/Wide-Angle X-ray Scattering Beam Line at the ESRF. *J. Appl. Crystallogr.* **2003**, *36*, 791–794.
- (31) Petukhov, A. V.; Thijssen, J. H. H.; 't Hart, D. C.; Imhof, A.; van Blaaderen, A.; Dolbnya, I. P.; Snigirev, A.; Moussaid, A.; Snigireva, I. Microradian X-ray Diffraction in Colloidal Photonic Crystals. *J. Appl. Crystallogr.* **2006**, *39*, 137–144.
- (32) van den Pol, E.; Thies-Weesie, D. M. E.; Petukhov, A. V.; Vroege, G. J.; Kvashnina, K. Influence of Polydispersity on the Phase Behavior of Colloidal Goethite. *J. Chem. Phys.* **2008**, *129*, 164715.
- (33) Aarts, D. G. A. L. The Interface in Demixed Colloid–Polymer Systems: Wetting, Waves and Droplets. *Soft Matter* **2007**, *3*, 19–23.